Predicting the Phase Behavior of Nitrogen + *n*-Alkanes for Enhanced Oil Recovery from the SAFT-VR Approach: Examining the Effect of the Quadrupole Moment

Honggang Zhao,[†] Pedro Morgado,[†,‡] Alejandro Gil-Villegas,[§] and Clare McCabe*[,†]

Department of Chemical Engineering, Vanderbilt University, Nashville, Tennessee 37235-1604, Centro de Química Estrutural, Instituto Superior Técnico, 1049-001 Lisboa, Portugal, and Instituto de Física, Universidad de Guanajuato, Léon 37150, México

Received: June 3, 2006; In Final Form: September 10, 2006

The phase behavior of nitrogen + *n*-alkanes is studied within the framework of the statistical associating fluid theory for potentials of variable range (SAFT-VR). The effect of the quadrupole moment of nitrogen on the phase behavior is considered through an extension of the SAFT-VR equation that includes an additional contribution to the Helmholtz free energy due to quadrupolar interactions. A significant improvement in the description of the phase diagram of the binary mixtures of nitrogen with different *n*-alkanes is obtained with the new approach when compared to predictions from the original SAFT-VR EOS (i.e., without the quadrupolar term). The experimental value for the quadrupole moment of nitrogen is used in the new equation; thus, no additional parameters are employed. Given the nonideal nature of the binary mixtures, a binary interaction parameter is needed to describe the full-phase diagram and high-pressure critical lines of these systems; however, this can be fitted to a single system and successfully used to predict the phase behavior of other binary mixtures without additional fitting. Furthermore, only a single, transferable, cross-energy parameter is required when the quadrupolar term is considered, whereas a cross-range parameter is also needed with the original SAFT-VR approach. The inclusion of the quadrupolar term in the equation of state therefore reduces the need to use effective parameters by explicitly including at the molecular level interactions due to the quadrupole moment.

1. Introduction

As supplies of oil and gas dwindle, enhanced recovery methods that can recover the remaining 40−60% of the original oil in a field become increasingly attractive. The most promising of these are thermal, chemical, and miscible recovery methods. Miscible oil displacement, as its name suggests, involves the displacement of oil by fluids with which it mixes in all proportions. Generally, a gas such as carbon dioxide or nitrogen is used and is continually injected into the reservoir, extracted back out with the recovered oil, recaptured, and re-injected along with new gas until as much oil as possible has been produced. The use of carbon dioxide for enhanced recovery techniques can be expensive compared to that of nitrogen if a source of carbon dioxide is not readily available; however, nitrogen requires a higher injection pressure to achieve miscibility with the reservoir fluids than does carbon dioxide. Nitrogen is therefore more commonly used in deep reservoirs. To optimize recovery strategies, reliable predictions for the thermodynamics and vapor−liquid equilibrium (VLE) of nitrogen/oil systems, such as knowledge of the minimum pressure required for miscibility, are needed. Toward this goal we present results for the prediction of nitrogen + alkane phase behavior using the SAFT-VR equation of state.[1,2] In particular, in an effort to develop a more predictive approach, we have investigated the impact of the quadrupole moment of nitrogen on the phase behavior.

Experimental studies of the phase behavior of nitrogen + alkane systems have shown that their binary mixtures exhibit different kinds of phase behavior, depending upon the length of the *n*-alkane chain. A transition is observed from simple type I (according to the classification scheme of van Konynenburg and Scott[3,4]) phase behavior for the nitrogen + methane binary mixture to type III for nitrogen + ethane and longer *n*-alkanes. The strong nonideality exhibited as chain length increases makes it difficult to accurately predict the phase diagrams of these systems using equations of state; typically a correction to the usual Lorentz−Berthelot combining rules is needed to determine the cross interactions, and is generally fitted to experimental data. Several equations of state, mostly cubic, have been used to describe the phase behavior of these systems, and alternative methods for determining the binary interaction parameters have been suggested. For example, Graboski and Daubert[5,6] correlated the binary interaction parameters used in the Soave−Redlich−Kwong (SRK) EOS in terms of the absolute difference in the solubility parameter of the two components; Nishiumi et al.[7] reported an expression for the binary interaction parameter used in the Peng−Robinson EOS in terms of the ratio of the critical molar volumes of the two components; and Moysan[8] studied the effect of temperature and solvent on the value of binary interaction coefficients in the SRK EOS. In each of these studies effective parameters are used to describe the effects of molecular shape and molecular interactions, and so the mixture parameters tend to have limited applicability beyond the systems and region of the phase diagram to which they were fitted.

To develop a more reliable and predictive approach the effects of the molecular shape and interactions need to be directly included into the equation of state. For this reason, molecular

* To whom correspondence should be addressed. E-mail: c.mccabe@vanderbilt.edu. Telephone: (615) 322-6853. Fax: (615) 343-7951.
[†] Vanderbilt University.
[‡] Instituto Superior Técnico.
[§] Universidad de Guanajuato.

10.1021/jp063444b CCC: $33.50
Published on Web 11/09/2006

based equations of state, such as the SAFT[9−11] equation, have gained popularity in both academic and industrial settings. An important feature of the SAFT approach, which is based on the thermodynamic perturbation of theory of Wertheim,[12−15] is that it explicitly takes into account nonsphericity and association interactions and provides a powerful method for investigating the phase behavior of both nonassociating and associating chain fluids. In the SAFT framework, the free energy is written as the sum of four separate contributions:

$$\frac{A}{NkT} = \frac{A^{\text{ideal}}}{NkT} + \frac{A^{\text{mono.}}}{NkT} + \frac{A^{\text{chain}}}{NkT} + \frac{A^{\text{assoc.}}}{NkT} \qquad (1)$$

where N is the number of molecules, k Boltzmann's constant, and T the temperature. A^{ideal} is the ideal free energy, $A^{\text{mono.}}$ the contribution to the free energy due to the monomer segments, A^{chain} the contribution due to the formation of bonds between monomer segments, and $A^{\text{assoc.}}$ is the contribution due to association. Hence, a SAFT fluid is a collection of monomers that can form covalent bonds; the monomers can interact via repulsive and attractive (dispersion) forces and, in some cases, association interactions. The many different versions of SAFT essentially correspond to different choices for the monomer fluid and different theoretical approaches to the calculation of the monomer free energy and structure.[16,17] Perhaps the most popular are the perturbed-chain and variable range versions of the SAFT approach (PC-SAFT and SAFT-VR, respectively). In the case of the PC-SAFT EOS,[18] monomers interact through a discrete potential proposed by Chen and Kreglewski,[19] the main feature of which is the use of a softened repulsive interaction. García-Sánchez et al.[20] have applied the PC-SAFT EOS to study the phase behavior of nitrogen + hydrocarbon mixtures, obtaining good results in comparison with experimental data when binary interaction parameters fitted to experimental data for each nitrogen + alkane system studied were used.

In this work we focus on using the SAFT-VR[1] approach to study the phase behavior of nitrogen + alkane systems and examining the effect of incorporating the quadrupolar interactions into to the equation of state. The SAFT-VR equation has been successfully used to describe the phase equilibria of a wide range of industrially important systems and provides a significant improvement in predictive capability over earlier formulations. For example, alkanes of low molecular weight through to simple polymers,[21−26] and their binary mixtures,[22,27−32] perfluoroalkanes,[33,34] hydrogen fluoride,[35] water,[36] refrigerant systems,[37] carbon dioxide,[31,38−41] electrolyte solutions,[42−44] and asphaltene precipitation[45] have all been studied. In the SAFT-VR approach,[1] the monomer−monomer interaction is described by a potential of variable range that can be modeled by different functional forms, such as a square-well or Yukawa interaction, and the dispersive interactions are treated via a second-order high-temperature perturbation expansion providing a more rigorous description of the thermodynamics than is found in simpler versions of the SAFT approach.[21] The SAFT-VR approach has recently been extended to accurately model the critical region[25,26,31,32] and rigorously incorporate dipolar interactions into the model chain.[85] In the original SAFT-VR approach polar interactions are taken into account in an effective way through the use of a variable ranged potential, without requiring knowledge of the values of multipolar moments. However, when both the dispersion and polar interactions are described by the variable range potential, this leads to effective parameters to describe the molecular interactions. To develop a more predictive approach it is desirable to have the polar interactions as an explicit contribution in the equation of state.

Perturbation theories can be extended to include polar interactions. The main difference, compared to perturbation theories developed for van der Waals forces, is that for perturbation theories developed in terms of the pair potential (as opposed to the Mayer f-function) there is no contribution to the first-order perturbation term in a high-temperature expansion (HTE) for a polar fluid if the reference-system pair interaction is spherically symmetric. The leading polar contributions in a HTE are given by the second- and third-order terms,[46,47] which can be used within a Padé approximant to predict the other perturbation terms. This approach is due to Stell et al.[46,48] and has provided a fundamental framework for further developments in the field of theoretical equations of state for polar substances. Gubbins and Twu,[49] on the basis of Stell's perturbation theory and the molecular dynamics simulation results of Verlet,[50] proposed a set of expressions to account for dipolar and quadrupolar interactions. The quadrupolar interaction was subsequently used by Donohue et al.[51] to describe quadrupolar fluids within the perturbed hard-chain theory (PHCT) approach.[52] An empirical dipole−dipole and quadrupole−quadrupole term for the two-center Lennard-Jones plus point polar fluid was later proposed by Saager et al.[53] from a fit to simulation data and applied to real fluids and mixtures. More recently, Gross[54] proposed a third-order perturbation theory contribution fitted to simulation data for the two-center Lennard-Jones plus point quadrupole fluid. The new term was combined with the PC-SAFT equation and used to study pure components and mixture, where the new equation was found to yield improvements for mixtures of a quadrupolar component with nonpolar solvents.

Of particular relevance to the proposed work is that of Benavides and co-workers,[55−57] who developed a perturbation theory for pure polar fluids, the so-called multipolar square-well theoretical equation of state (MSWTEOS), that is based on an accurate equation of state for square-well fluids due to Gil-Villegas et al.[58] and Stell's Padé expression for the polar contribution to the Helmholtz free energy. This theory has been successful in describing the vapor- and liquid-phase properties of pure systems such as methane, nitrogen, water, and carbon dioxide.[59−61] In this work, we extend the SAFT-VR equation by incorporating a quadrupolar contribution into the expression for the Helmholtz free energy that is based on an extension of the framework developed in the MSWTEOS to mixtures of chain molecules. The modified SAFT-VR equation obtained is then applied to study the phase behavior of nitrogen and its binary mixtures with the n-alkanes. Results are compared with the predictions obtained from the original SAFT-VR EOS and experimental data. The remainder of the paper is organized as follows: in section 2 we present the quadrupolar SAFT-VR approach; in section 3, results for the phase behavior of pure nitrogen and binary mixtures of nitrogen with alkanes are presented; finally, concluding remarks are made, and future work is discussed in section 4.

2. Molecular Models and Theory

We use the SAFT-VR model for the n-alkanes,[1,23] which has been shown in previous work to provide a very good description of the vapor pressure and coexisting densities of n-alkanes. To summarize, alkane molecules are modeled as chains of m tangentially bonded monomer segments each described by three parameters; the diameter of the hard sphere segments σ, and the depth ϵ and range λ of the square-well potential characterizing the attractive dispersion interaction between segments. The number of segments in the model chain is determined from the

number of carbon atoms C in the molecule according to $m = (C - 1)/3 + 1.0$. In our approach, nitrogen is described as a chain molecule with a net point axial quadrupole moment located at the center of the molecule, for which the value of 4.55×10^{-40} $C \cdot m^2$ is used and is an average of experimentally reported values;[62] thus, no additional fitted parameter is needed for the description of the quadrupolar interactions.

In terms of the Helmholtz free energy, A, the equation of state for the nitrogen + n-alkane systems can be written as a sum of four separate contributions:

$$\frac{A}{NkT} = \frac{A^{\text{ideal}}}{NkT} + \frac{A^{\text{mono.}}}{NkT} + \frac{A^{\text{chain}}}{NkT} + \frac{A^{Q}}{NkT} \tag{2}$$

where the additional term (A^{Q}), in comparison with eq 1, represents the residual Helmholtz free energy due to the quadrupolar−quadrupolar interactions. Also we have not included the contribution due to association interactions in eq 2, since the fluids considered in this work consist of nonassociating molecules.

To extend the SAFT-VR approach to a theory that includes a quadrupolar contribution to the free energy, as expressed in eq 2, we consider chain molecules formed from monomer segments each with an axial quadrupolar moment in such a way that the addition of these moments gives the experimental value of the quadrupolar moment. If we have a chain molecule formed by m segments and define Q as the total quadrupolar moment, each segment has a quadrupolar moment of Q/m. This result is an extension of the definition of center of charges, assuming that the chain molecular axis, where we are locating the net axial quadrupole, and each one of the segment axis are parallel to each other, since the quadrupolar moment is a tensorial property that can be added as a scalar quantity only in this case. This result also applies to the moment of inertia, another tensorial property that can be added as a scalar if the rotation axis is the same for all the considered segments. Notice that this restriction of segment axis parallel to molecular axis is exact only for diatomics and will be an approximation for longer chains. This is because for linear molecules with more than two centers, the molecule is generally flexible, and so the vectors between the segments are no longer collinear (many conformations will result in their not being collinear). Hence, in the case of linear n-mers where $n > 2$ the scalar quadrupole moment of the molecule cannot be represented exactly as a sum of the scalar quadrupole moment of the individual segments.

Following this result, we consider chain molecules formed from monomer segments that interact through a square-well potential of variable range, U_{ij}^{SW}, together with a quadrupolar interaction, U_{ij}^{QQ}, i.e.,

$$U_{ij}(r,\Omega_1,\Omega_2) = U_{ij}^{\text{SW}}(r;\sigma,\lambda,\epsilon) + U_{ij}^{\text{QQ}}(r,\Omega_1,\Omega_2;\sigma,Q/m) \tag{3}$$

where

$$U_{ij}^{\text{SW}} = \begin{cases} +\infty & \text{if } r < \sigma_{ij} \\ -\epsilon_{ij} & \text{if } \sigma_{ij} \le r < \lambda_{ij}\sigma_{ij} \\ 0 & \text{if } r \ge \lambda_{ij}\sigma_{ij} \end{cases} \tag{4}$$

and σ_{ij} is the diameter of the hard-spheres interaction, λ_{ij}, the range, and ϵ_{ij}, the well depth of the SW potential, and

$$U_{ij}^{QQ} = \frac{3\Gamma_{ij}}{4r^5}\Psi(\Omega_1,\Omega_2) \tag{5}$$

with

$$\Psi(\Omega_1,\Omega_2) = 1 - 5(c_1^2 + c_2^2) - 15c_1^2c_2^2 + 2(s_1s_2c - 4c_1c_2)^2 \tag{6}$$

where $c_1 = \cos\theta_1$, $c_2 = \cos\theta_2$, $s_1 = \sin\theta_1$, $s_2 = \sin\theta_2$, $c = \cos(\phi_1 - \phi_2)$, $\Omega_i = \{\theta_i,\phi_i\}$ are the polar and azimuthal angles of segment i of the linear charge distribution with respect to the line connecting the molecular centers, and Γ_{ij} is the segment quadrupole moment.

The inter- and intramolecular cross interactions between segments are obtained from the standard combining rules, viz.

$$\sigma_{ij} = \frac{\sigma_{ii} + \sigma_{jj}}{2} \tag{7}$$

$$\epsilon_{ij} = (1 - k_{ij})(\epsilon_{ii}\epsilon_{jj})^{1/2} \tag{8}$$

$$\lambda_{ij} = (1 - \gamma_{ij})\left(\frac{\lambda_{ii}\sigma_{ii} + \lambda_{jj}\sigma_{jj}}{\sigma_{ii} + \sigma_{jj}}\right) \tag{9}$$

where k_{ij} and γ_{ij} are binary interaction parameters that are fitted to experimental data to improve the Lorentz−Berthelot rules. In systems with more than one quadrupolar component an additional relationship is needed,

$$\Gamma_{ij} = \sqrt{\frac{Q_iQ_j}{m_im_j}} \tag{10}$$

Following the SAFT-VR approach applied to the system defined by the pair interaction given previously (eq 3), we now briefly summarize the main expressions for each contribution to the Helmholtz free energy in eq 2. Detailed expressions for the quadrupolar term are given below, while those for the remaining terms are given in the appendix.

The monomer free energy due to the SW pair interaction, eq 4, is given by,

$$\frac{A^{\text{mono.}}}{NkT} = (\sum_{x=1}^{n} x_i m_i)\frac{A^{\text{M}}}{N_s kT} = (\sum_{x=1}^{n} x_i m_i)a^{\text{M}} \tag{11}$$

where N_s is the total number of segments, determined from the product of the total number of molecules N and the number of segments per molecule m_i; a^{M} is the free energy per monomer segment, and in the SAFT-VR equation a^{M} is approximated by a second-order high-temperature expansion using Barker and Henderson perturbation theory for mixtures,[63] viz.

$$a^{\text{M}} = a^{\text{HS}} + \beta a_1 + \beta^2 a_2 \tag{12}$$

where $\beta = 1/kT$, a^{HS} is the free energy of the hard sphere reference fluid and a_1 and a_2 are the first and second perturbation terms, respectively. The Helmholtz free energy of the hard sphere reference fluid is determined from the expression of Boublik[64] and Mansoori et al.,[65] and the perturbation terms are expressed in terms of the contact value of the HS radial distribution function and an effective packing fraction (see Appendix A and ref 2)

For the quadrupolar term, following the discussion above, we apply Stell's Padé approximant to develop a simple model that can be extended to mixtures in a straightforward manner, viz.

$$\frac{A^{Q}}{NKT} = m\frac{A^{Q}}{N_s KT} = ma^{Q} = m\frac{a_3^{Q}}{1 - a_3^{Q}/a_2^{Q}} \tag{13}$$

where the terms a_2^Q and a_3^Q correspond to the second- and third-order perturbation terms for a quadrupolar fluid when a HS fluid is used as a reference system. The first-order term, a_1^Q, is null, as discussed previously. According to Larsen et al.[66] we have the following expressions for the polar perturbation terms:

$$a_2^{Q} = -\frac{7}{10}\rho^*_s Q^{*4}\beta^2 F_1$$

$$a_3^{Q} = Q^{*6}\beta^3\left[\frac{36}{245}\rho^*_s F_2 + \frac{1}{6400}\rho_s^{*2} F_3\right] \tag{14}$$

where the reduced quadrupolar moment is defined as

$$Q^* = \frac{Q}{m\sqrt{\epsilon\sigma^5}}$$

and

$$m = \sum_{i=1}^{n} x_i m_i$$

and F_1, F_2, and F_3 are functions of density, given by

$$F_1 = 1.7952 + 1.755\rho_s^* + 1.0376\rho_s^{*2} + 0.3890\rho_s^{*3} + 0.1561\rho_s^{*4} - 0.0082\rho_s^{*5}$$

$$F_2 = 1.0472 + 1.1631\rho_s^* + 0.8552\rho_s^{*2} + 0.4506\rho_s^{*3} + 0.1913\rho_s^{*4} + 0.1465\rho_s^{*5}$$

$$F_3 = 532.9586 + 1287.3491\rho_s^* + 1533.95426\rho_s^{*2} + 1110.5044\rho_s^{*3} + 720.1578\rho_s^{*4} - 248.8879\rho_s^{*5} \tag{15}$$

It is straightforward to extend the quadrupole term to mixtures using the following mixing rules,

$$Q^* = \sum_i \sum_j x_{si} x_{sj} Q_{ij}^*$$

$$Q_{ij}^* = \sqrt{Q_i^* Q_j^*} \tag{16}$$

Notice that according to the definition given for the segment quadrupole moment and the expression for A^Q given by eq 13, the monomer free energy will be given by the sum of the SW and polar contributions, and hence eq 11 can be rewritten,

$$\frac{A^{\text{mono.}}}{NkT} = \left(\sum_{i=1}^{n} x_i m_i\right)\left[a_{\text{HS}} + \beta a_1 + \beta^2 a_2 + \frac{a_3^{Q}}{1 - \dfrac{a_3^{Q}}{a_2^{Q}}}\right] \tag{17}$$

and the expression in square brackets reduces to the MSWTEOS for a quadrupolar pure-component fluid. Following Benavides et al., the perturbation expansion in powers of β for a monomeric quadrupolar SW fluid has a first-order term a_1, which corresponds to the SW contribution, and a second-order term that is exactly given by the sum of the corresponding fluctuation terms for a SW fluid and a HS quadrupolar fluid, respectively. The third-order term, however, not only is the sum of the corresponding SW and quadrupolar free energies but also contains a cross SW-quadrupole contribution, a^{Q+SW}. This last term involves three separated contributions that require the use of two-, three-, and four-body correlation functions for the HS fluid. Due to the lack of knowledge of these functions in the MSWTEOS, a^{Q+SW} is neglected. In the case of the theory developed in this work, the same approximation has been used. However, due to nature of the SAFT-VR equation, the contribution of the cross SW-polar energy term is effectively accounted for by the use of a variable range SW potential. As has been discussed in previous work on electrolyte solutions modeled with the SAFT-VR approach, the effect of neglecting information that is present in real systems can be incorporated in an effective way in variable range systems. This approximation was first recognized by Debye and Huckel,[67] and later by Stell and co-workers[68] for ionic and polar fluids in their generalized mean spherical approximation (GMSA) theory. This important feature of the SAFT-VR approach also has an effect in the evaluation of the contact value of the radial distribution function, as discussed below.

Considering our segments as SW + quadrupole monomers, the contribution due to chain formation from the quadrupolar SW segments is given in terms of the angular average of the background correlation function, $y_{ii}^{QSW}(r,\Omega_1,\Omega_2)$,

$$\frac{A^{\text{chain}}}{NkT} = -\sum_{i=1}^{n} x_i(m_i - 1)\ln\langle y_{ii}^{QSW}(\sigma_{ii},\Omega_1,\Omega_2)\rangle \tag{18}$$

where

$$y_{ii}^{QSW}(\sigma_{ii},\Omega_1,\Omega_2) = \exp\beta\left[-\epsilon_{ii} + \frac{3Q_{ii}^2\Psi(\Omega_1,\Omega_2)}{4m_i^2\sigma_{ii}^5}\right] g_{ii}^{QSW}(\sigma_{ii},\Omega_1,\Omega_2) \tag{19}$$

since, by definition, $y = e^{\beta u}g$, and $g_{ii}^{QSW}(\sigma_{ij},\Omega_1,\Omega_2)$ is the pair correlation function for a quadrupolar SW fluid. Applying an angular average in eq 19 we obtain,

$$\langle y_{ii}^{QSW}(\sigma_{ii},\Omega_1,\Omega_2)\rangle = e^{-\beta\epsilon_{ii}}\left\langle \exp\left[\frac{3\beta Q_{ii}^2\Psi(\Omega_1,\Omega_2)}{4m_i^2\sigma_{ii}^5}\right] g_{ii}^{QSW}(\sigma_{ii},\Omega_1,\Omega_2)\right\rangle \tag{20}$$

Since the exponential term and the pair correlation function are always positive, the conditions required to apply the generalized mean value theorem are satisfied, and we choose the exponential term to be factored outside the angular average evaluated at orientations Ω_1^*,Ω_2^*. Equation 20 is then evaluated as

$$\langle y_{ii}^{QSW}(\sigma_{ii},\Omega_1,\Omega_2)\rangle = e^{-\beta\epsilon_{ii}}\exp\left[\frac{3\beta Q_{ii}^2\Psi(\Omega_1^*,\Omega_2^*)}{4m_i^2\sigma_{ii}^5}\right]\langle g_{ii}^{QSW}(\sigma_{ii},\Omega_1,\Omega_2)\rangle \tag{21}$$

Using eq 21 in eq 18, we obtain

$$\frac{A^{\text{chain}}}{NkT} = -\sum_{i=1}^{n} x_i(m_i - 1)\ln\langle g_{ii}^{QSW}(\sigma_{ii},\Omega_1,\Omega_2)\rangle + \sum_{i=1}^{n} x_i(m_i - 1)\beta\left[\epsilon_{ii} - \frac{3Q_{ii}^2\Psi(\Omega_1^*,\Omega_2^*)}{4m_i^2\sigma_{ii}^5}\right] \tag{22}$$

The function $g_{ii}^{QSW}(\sigma_{ij},\Omega_1,\Omega_2)$ is approximated by a first-order

TABLE 1: Optimized and Rescaled Square-Well Intermolecular Potential Parameters for Nitrogen for the Original SAFT-VR Approach and the Quadrupolar SAFT-VR Approach[a]

σ/Å	$(\epsilon/k)K$	λ	m	$Q(\times 10^{-40}\ C\cdot m^2)$	σ_c/Å	$(\epsilon_c/k)K$
3.1477	73.2092	1.5999	1.33	4.55	3.3685	71.0358
3.1588	81.4851	1.55	1.33	0.0	3.4237	77.2536

[a] σ is the diameter of each segment, ϵ the potential well depth, λ the potential range, m the number of spherical segments in the model, and Q the quadrupole moment. The subscript c indicates those parameters that have been rescaled to the experimenal critical point of pure nitrogen ($T_c = 126.91$ K $P_c = 3.39$ MPa).

high-temperature perturbation expansion around a HS reference system:

$$g_{ii}^{QSW}(\sigma_{ij},\Omega_1,\Omega_2) = g_{ij}^{HS}(\sigma_{ij}) + \beta\epsilon_{ii}g_1^{QSW}(\sigma_{ij},\Omega_1,\Omega_2) \qquad (23)$$

Following the SAFT-VR method for the calculation of the contact value of the first-order perturbation term of the pair-correlation function, g_1^{QSW} is determined using a self-consistent method between the pressure obtained by applying the Clausius virial theorem and the pressure obtained from the derivative of the Helmholtz free energy with respect to the density.[1] Requiring that both pressures have equal values for any density and temperature, we calculate that there is no explicit polar contribution to g_1^{QSW} as a consequence of the zero contribution to the mean-attractive energy for the polar-pair interaction. Therefore, $g_1^{QSW}(\sigma_{ii}) = g_1^{SW}(\sigma_{ii})$, where

$$g_1^{SW}(\sigma_{ij}) = \frac{1}{2\pi\epsilon_{ij}\sigma_{ij}^3}\left[3\left(\frac{\partial(a_1)_{ij}}{\partial\rho_s}\right) - \frac{\lambda_{ij}}{\rho_s}\frac{\partial(a_1)_{ij}}{\partial\lambda_{ij}}\right] \qquad (24)$$

We want to stress here that eq 22 does not mean that the chain contribution energy of eq 18 is independent of any polar information, an apparent contradiction since we are dealing with a property of segments that are indeed polar. In this work, the variable range SW system is taking into account the effect of the structure of the polar segments.

3. Results and Discussion

The SAFT-VR parameters for nitrogen, excluding the quadrupole moment for which the experimental value is used, were determined from a fit to the experimental vapor pressure and saturated liquid density. The parameters for nitrogen, both with and without the quadrupole term, are presented in Table 1. We note from these parameters that for the same value of the number of segments per chain ($m = 1.33$) the use of a quadrupole moment reduces the depth of the square well (ϵ), with respect to the model without the quadrupole, while increasing the value of the attractive range (λ). The contribution to the dispersion forces is therefore approximately the same for both models, which can be seen if we consider the van der Waals attractive constant (eq A-7 in Appendix A). If α and α_Q are the van der Waals constant for the models with and without the quadrupole respectively, we find that $\alpha/\alpha_Q = 0.9899$, indicating that both systems essentially have the same dispersive contribution to the free energy.

In Figure 1 we present the SAFT-VR descriptions, both with and without the quadrupole term, for the vapor pressure curve and coexisting densities of nitrogen, in comparison with experimental data. From Figure 1 we can see that, although both approaches provide a good description of the phase behavior

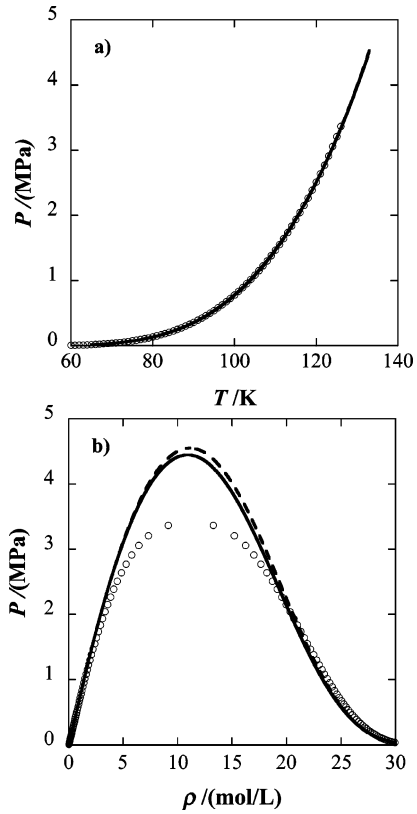

Figure 1. (a) Vapor pressure and (b) coexisting densities for nitrogen. Solid line represents predictions from the quadrupolar SAFT-VR approach, dashed line, results from the original SAFT-VR equation, and circles, the experimental data taken from ref 70.

of nitrogen, an improvement in the description of the coexisting densities when the quadrupole is included into the theory is observed, whereas the prediction of the vapor pressures is slightly more accurate without the quadrupole. In common with essentially all analytical equations of state, both approaches over-predict the critical point of nitrogen due to the negligence of the long-range fluctuations in the density in the vicinity of the critical point, which has been addressed in other work.[25,26,31,32] If one is interested in the critical region of the phase diagram, the parameters optimized against experimental data can be rescaled to the experimental critical point in order to reproduce the experimental critical temperature and pressure and allow the study of the critical lines. While not as rigorous as incorporating the effects of the scaling behavior, seen in the vicinity of the critical point, into the theory, rescaling does provide an easy way to determine parameters that can be used to study the critical region. The rescaled parameters for nitrogen are also presented in Table 1, and the vapor pressures and coexisting densities of nitrogen obtained from the SAFT-VR equation with rescaled parameters, with and without the quadrupole term, are compared with experimental data in Figure 2. With the rescaled parameters, both approaches are seen to accurately describe the vapor pressure of nitrogen, with a slight deviation being observed at lower temperatures (a direct consequence of the rescaled parameters).

To investigate the effect of the quadrupole on the mixture phase behavior of nitrogen we have used the SAFT-VR equation, with and without the quadrupole term, to predict the phase diagrams of nitrogen + *n*-alkane binary mixtures from methane to *n*-decane. In Figure 3 we present a comparison of experimental constant temperature $p-x$ slices for the methane (1) + nitrogen (2) phase diagram with theoretical results from

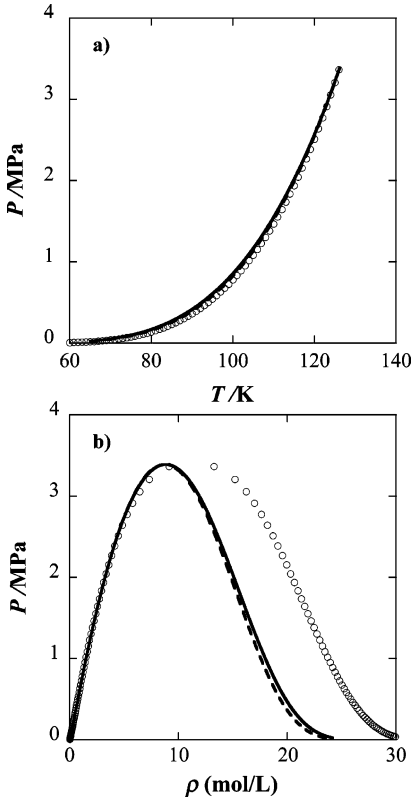

Figure 2. (a) Vapor pressure and (b) coexisting densities of nitrogen compared with theoretical results using rescaled parameters. Solid line represents predictions from the quadrupolar SAFT-VR approach, dashed line, results from the original SAFT-VR equation, and circles, the experimental data taken from ref 70.

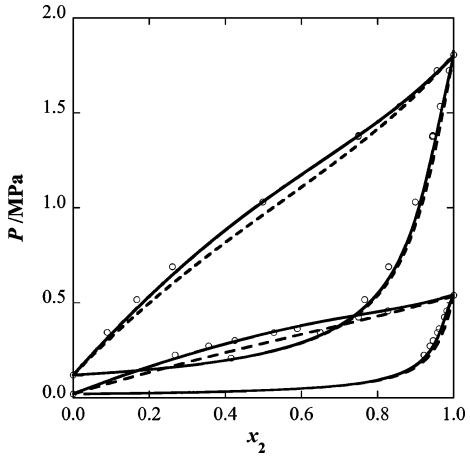

Figure 3. Constant temperature $p-x$ slices of the phase diagram for the methane (1) + nitrogen (2) binary mixture at 95 and 113.7 K (from bottom to top). The continuous curves correspond to predictions from the quadrupolar SAFT-VR equation, and the dashed curves, from the original SAFT-VR approach. The circles represent the experimental results taken from refs 71 and 72.

the SAFT-VR equation, both with and without the quadrupolar term, at temperatures of 95 and 113.71 K. Using the simple Lorentz−Berthelot combining rules (i.e., $k_{ij} = 0$ and $\gamma_{ij} = 0$), both approaches predict the phase diagram very well, with the predicted result from the SAFT-VR equation with the quadrupolar term being in better agreement with the experimental data than the results from original SAFT-VR approach. The improved accuracy of the quadrupolar SAFT-VR equation is also seen when we consider longer chain lengths. In Figures 4 and 5 we

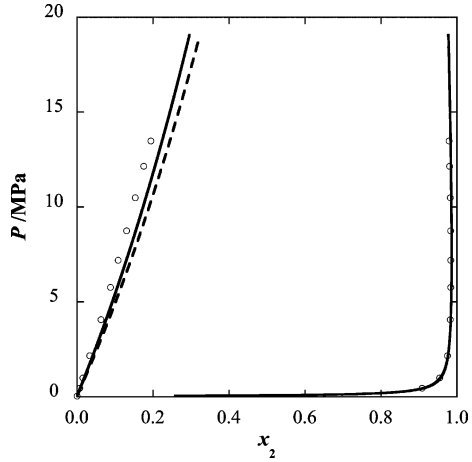

Figure 4. Constant temperature $p-x$ slices of the phase diagram for the butane (1) + nitrogen (2) binary mixture at 250 K. The continuous curves correspond to predictions from the quadrupolar SAFT-VR approach, and the dashed curves, predictions form the original SAFT-VR equation. The circles represent the experimental results taken from ref 73.

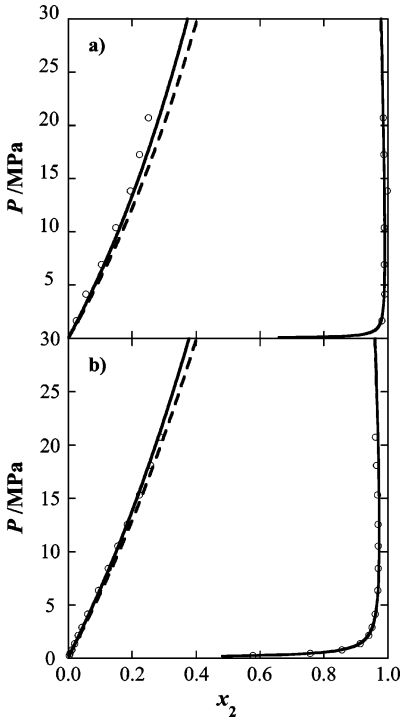

Figure 5. Constant temperature $p-x$ slices of the phase diagram for the pentane (1) + nitrogen (2) binary mixture at 277.43 and 310.7 K (from top to bottom). The continuous curves correspond to predictions from the quadrupolar SAFT-VR approach, and the dashed curves, predictions from the original SAFT-VR equation. The circles represent experimental data taken from ref 74.

present constant temperature slices of the phase diagram for the binary mixtures of butane (1) + nitrogen (2) and pentane (1) + nitrogen (2), calculated from both the quadrupolar SAFT-VR and original SAFT-VR approaches. The bubble point pressures calculated from the quadrupolar SAFT-VR equation are again in better agreement with the experimental data than those calculated with the original SAFT-VR approach. We note however that more significant deviations from the experimental data are observed for the nitrogen (1) + heptane (2) binary mixture, as shown in Figure 6. To obtain a better agreement with experimental data for this system, binary interaction

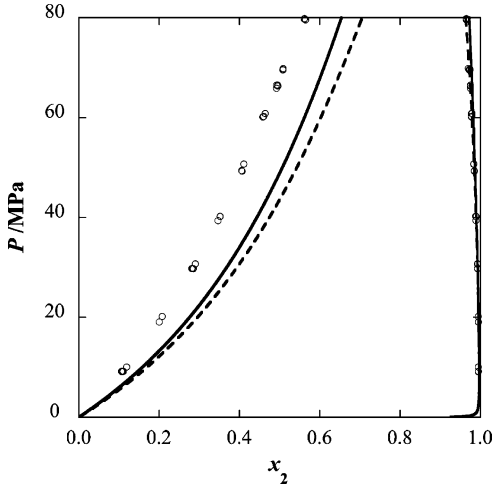

Figure 6. Constant temperature $p-x$ slices of the phase diagram for the heptane (1) + nitrogen (2) binary mixture at 305.4 K. The continuous curves correspond to predictions from the quadrupolar SAFT-VR approach, and the dashed curves, predictions from the original SAFT-VR equation. The circles are experimental results taken from ref 75.

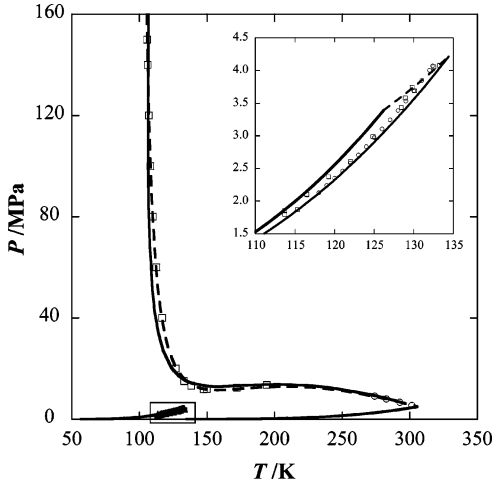

Figure 7. $p-T$ projection of the ethane (1) + nitrogen (2) phase diagram. The continuous curves correspond to predictions from the quadrupolar SAFT-VR approach, and the dashed curves, predictions from the original SAFT-VR equation. (Inset) Bold curves are the pure component vapor pressures, and the thin line represents the three-phase line. Results from the quadrupolar SAFT-VR equation are shown. The symbols represent experimental data taken from refs 76−80.

parameters, fitted to the mixture experimental data, would be needed for both the quadrupolar and the original SAFT-VR equations.

We have also studied the global fluid phase diagram and critical lines for several nitrogen + alkane binary mixtures, the choice depending upon the availability of experimental data. To describe the high-pressure critical lines we use the rescaled parameters for nitrogen (Table 1) and the alkanes.[23] As stated in the Introduction, the ethane + nitrogen binary system exhibits type-III phase behavior in the classification of Scott and van Konynenburg, thus exhibiting a noncontinuous critical line. As would be expected for this nonideal system, and based on earlier work with the SAFT-VR equation, deviations to the Lorentz−Berthelot combining rules need to be accounted for by introducing binary interaction parameters fitted to experimental data (k_{ij} and γ_{ij} in eqs 8 and 9, respectively). In the quadrupolar SAFT-VR approach, quantitative agreement is achieved by using a single fitted binary interaction parameter for the unlike square-well depth (k_{ij}). However, the original SAFT-VR equation requires adjustment of both the cross-depth (k_{ij}) and cross-range parameters (γ_{ij}) in order to obtain quantitative agreement with the experimental data. These parameters were determined by fitting to the high-pressure critical line for the ethane (1) + nitrogen (2) binary mixture. The values obtained were $k_{ij} = 0.0395$ for the quadrupolar SAFT-VR approach and $k_{ij} = 0.118$ and $\gamma_{ij} = -0.028$ for the original SAFT-VR equation. We note that the magnitude of the k_{ij} when the quadrupole is included in the equation of state is markedly smaller, indicating that the deviations from the Lorentz−Berthelot rules are less important when the quadrupole is taken into account in a direct way rather than through effective parameters. In Figure 7 we present the $p-T$ projection of the predicted phase diagram for the ethane (1) + nitrogen (2) binary mixture compared with experimental data. It can be seen that the agreement between the theoretical predictions and experimental data is very good with both approaches. Focusing on the inset of Figure 7, for which results for the quadrupolar SAFT-VR equation are shown, we note that the agreement with experimental data along the three-phase line is very good, particularly given that the binary interaction parameter was fitted to the high-pressure critical line. If we consider $p-x$ slices of the phase diagram, as shown in Figure 8, we can see that the predictions from the quadrupolar SAFT-VR approach are in better agreement with the experimental data than the original SAFT-VR equation.

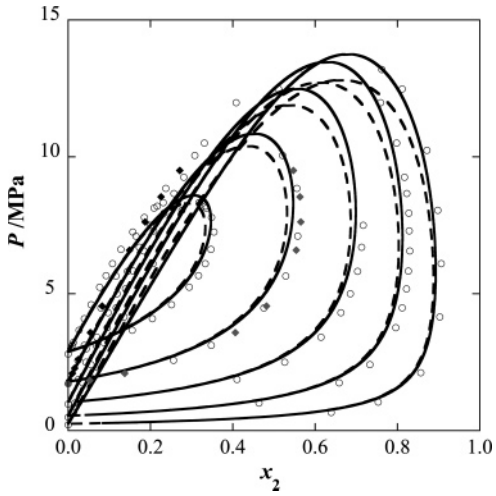

Figure 8. Constant temperature $p-x$ slices for the ethane (1) + nitrogen (2) binary mixture at 200 K, 220 K, 240, 260, and 280 K (from left to right). The solid lines represent predictions from the quadrupolar SAFT-VR approach with $k_{ij} = 0.0395$ and the dashed line predictions from the original SAFT-VR equation with $k_{ij} = 0.118$ and $\gamma_{ij} = -0.028$. The symbols are experimental data from refs 79, 81−83.

To test the transferability of the cross interaction parameters, the binary interaction parameters fitted to the high-pressure critical line of the ethane + nitrogen binary mixture have been used to predict the phase behavior of other alkane + nitrogen systems. In Figure 9 we present constant temperature $p-x$ slices of the phase diagram for the methane (1) + nitrogen (2) binary mixture. We note that both the original SAFT-VR and the quadrupolar SAFT-VR approaches correctly predict the transition from type-I (observed for methane + nitrogen) to type-III (observed for ethane + nitrogen) phase behavior using the transferable cross interaction parameters. When comparing the two approaches we find that the quadrupolar SAFT-VR equation is again in better agreement with the experimental data than the original SAFT-VR approach. If we consider longer chain lengths, in Figure 10 we present the high-pressure critical line for the pentane (1) + nitrogen (2) binary mixture. Again, we

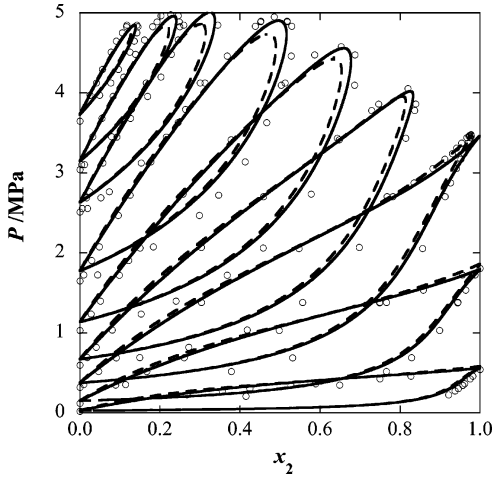

Figure 9. Constant temperature $p-x$ slices for the methane (1) + nitrogen (2) binary mixture at 95, 113, 127.59, 138.44, 149.82, 160.93, 172.04, 177.59, and 183.15 K (from bottom to top). The solid lines represent predictions from the quadrupolar SAFT-VR equation with $k_{ij} = 0.0395$, and the dashed line represents predictions from the original SAFT-VR approach with $k_{ij} = 0.118$ and $\gamma_{ij} = -0.028$. The symbols are experimental data taken from refs 71, 72.

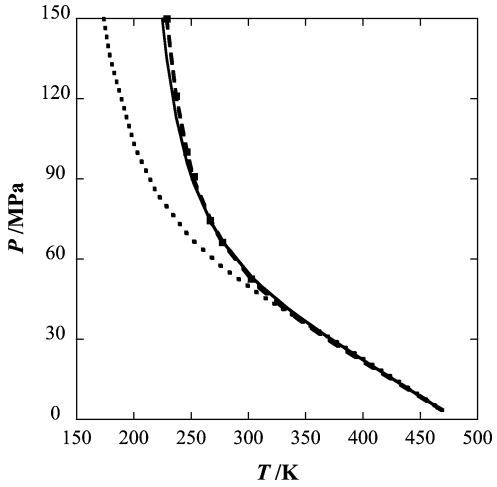

Figure 10. $p-T$ projection of the critical line for the pentane (1) + nitrogen (2) binary mixture. The continuous curves correspond to predictions from the quadrupolar SAFT-VR approach with $k_{ij} = 0.0395$, the dashed curves, predictions from the original SAFT-VR equation with $k_{ij} = 0.216$ and $\gamma_{ij} = -0.066$, and the dotted curves, the original SAFT-VR with $k_{ij} = 0.118$ and $\gamma_{ij} = -0.028$. The symbols are experimental data taken from ref 77.

find that the quadrupolar SAFT-VR approach provides a good prediction of the phase behavior using the binary interaction parameter fitted to the ethane + nitrogen system. However, we see a marked deviation between the experimental data and the theoretical predictions from the original SAFT-VR approach, although the shape of the curve is qualitatively correct; a new set of parameters ($k_{ij} = 0.216$ and $\gamma_{ij} = -0.066$) is needed to quantitatively describe the phase behavior with the original SAFT-VR approach. When we consider the decane (1) + nitrogen (2) system (Figure 11), the only other nitrogen + *n*-alkane system for which experimental data is available for a significant part of the critical line, the parameters fitted to the ethane + nitrogen critical line give only qualitative agreement with experimental data, not only with the original SAFT-VR approach but also for the quadrupolar SAFT-VR equation. In order to accurately describe the experimental data, a new set of binary interaction parameters must be determined for both

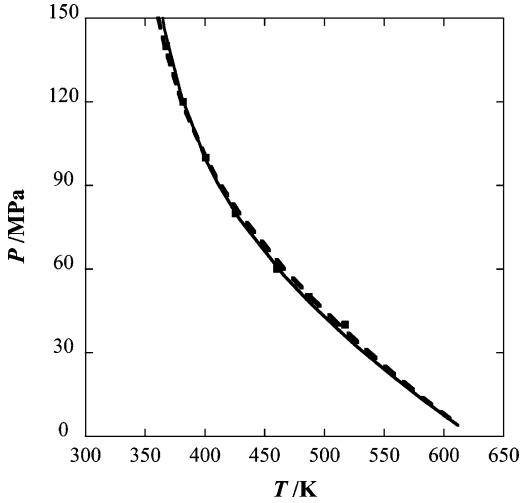

Figure 11. $p-T$ projection of the critical line for the decane (1) + nitrogen (2) binary mixture. The continuous curves correspond to predictions from the quadrupolar SAFT-VR equation with $k_{ij} = 0.285$ and $\gamma_{ij} = -0.089$), and the dashed curves, predictions from the original SAFT-VR equation with $k_{ij} = 0.289$ and $\gamma_{ij} = -0.089$. The symbols are experimental data taken from ref 84.

approaches, and for this system, the quadrupolar SAFT-VR approach also requires the use of two binary interaction parameters. This result suggests that the quadrupolar contribution becomes less relevant as the chain length of the alkane increases, i.e. the importance of the quadrupolar interaction in the nitrogen molecule is diminished and the dispersions forces become dominant as the chain length of the alkane increases.

Conclusions

The SAFT-VR equation of state was extended to account for quadrupolar interactions using a Pade-approximation term derived from perturbation theory. The new quadrupolar SAFT-VR approach was then applied to predict the phase diagrams of binary mixtures of alkanes with nitrogen and compared directly with the original SAFT-VR equation and with experimental data. The quadrupolar SAFT-VR equation is found to be in better agreement with experimental data. This is particularly encouraging, given the simplicity of the quadrupolar term and the fact that the experimental value of the quadrupole moment is used (i.e. an additional adjustable parameter is not added to the theory). Furthermore in the study of the high-pressure critical lines of these systems, the quadrupolar SAFT-VR approach only requires a single binary interaction parameter for most systems studied (all except C_{10}), compared to two binary interaction parameters for the original SAFT-VR approach. We can therefore conclude that inclusion of the quadrupolar interaction into the SAFT-VR equation improves the predictive ability of the SAFT-VR EOS when studying the phase behavior of alkane + nitrogen systems and reduces the need to use effective parameters by explicitly including at the molecular level interactions due to the quadrupole moment.

Acknowledgment. H.G. and C.M.C. acknowledge financial support from the National Science Foundation under Grant Number CTS-0453229. A.G.V. acknowledges financial support from CONACYT Grant Numbers 2003-C03-42439/A-1 and 41678-F. P.M. gratefully acknowledges the Fulbright Commission and the Luso-American Foundation for financially supporting his visit to the U.S. We acknowledge Ana Laura Benavides, Yolanda Guevara, and Eduardo Filipe for useful discussions.

Appendix A

We present here the main expressions for each contribution to the Helmholtz free energy within the framework of the SAFT-VR approach.

Ideal Contribution. The ideal contribution to the free energy is expressed as:

$$\frac{A^{\text{ideal}}}{NkT} = \sum_{i=1}^{n} x_i \ln(\rho_i \Lambda_i^3) - 1 = x_1 \ln(\rho_1 \Lambda_1^3) + x_2 \ln(\rho_2 \Lambda_2^3) - 1 \quad \text{(A-1)}$$

where $\rho_i = N_i/V$ the number density and Λ_i, the thermal de Broglie wavelength of species i.

SW Monomer Contribution. The hard sphere reference term a^{HS} is determined from the expression of Boublik[64] and Mansoori and co-workers[65] for multicomponent hard sphere systems, viz.

$$a^{\text{HS}} = \frac{6}{\pi\rho_s}\left[\left(\frac{\zeta_2^3}{\zeta_3^2} - \zeta_0\right)\ln(1-\zeta_3) + \frac{3\zeta_1\zeta_2}{1-\zeta_3} + \frac{\zeta_2^3}{\zeta_3(1-\zeta_3)^2}\right] \quad \text{(A-2)}$$

where ρ_s is the number density of segments, which is defined as the total number of segments divided by the total volume N_s/V and ζ_l is the reduced density given by a sum over all segments i,

$$\zeta_l = \frac{\pi}{6}\rho_s\left[\sum_{i=1}^{n} x_{s,i}(\sigma_i)^l\right] = \frac{\pi}{6}\rho_s[x_{s,1}(\sigma_1)^l + x_{s,2}(\sigma_2)^l] \quad \text{(A-3)}$$

where σ_i is diameter of segments of type i and $x_{s,i}$ is the mole fraction of segments in the mixture given by

$$x_{s,i} = \frac{m_i x_i}{\sum_{k=1}^{n} m_k x_k} = \frac{m_i x_i}{m_1 x_1 + m_2 x_2} \quad \text{(A-4)}$$

The first perturbation term a_1 describing the mean attractive energy is obtained from the sum of all pair interactions,

$$a_1 = \sum_{i=1}^{n}\sum_{j=1}^{n} x_{s,i}x_{s,j}(a_1)_{ij} = x_{s,1}^2(a_1)_{11} + 2x_{s,1}x_{s,2}(a_1)_{12} + x_{s,2}^2(a_1)_{22} \quad \text{(A-5)}$$

where $(a_1)_{ij}$ is obtained from the generalized mean-value theorem,

$$(a_1)_{ij} = -2\pi\rho_s\epsilon_{ij}\int_{\sigma_{ij}}^{\infty} r_{ij}^2 g_{ij}^{HS}(r_{ij})dr_{ij} = -\rho_s\alpha_{ij}^{\text{VDW}} g_{ij}^{\text{HS}}(\sigma_{ij};\zeta_3^{\text{eff}}) \quad \text{(A-6)}$$

where

$$\alpha_{ij}^{\text{VDW}} = \frac{2\pi}{3}\sigma_{ij}^3\epsilon_{ij}(\lambda_{ij}^3 - 1) \quad \text{(A-7)}$$

Within the van der Waals one-fluid theory the radial distribution function $g_{ij}^{\text{HS}}(\sigma_{ij};\zeta_3^{\text{eff}})$ is approximated by that for a pure fluid, viz.

$$(a_1)_{ij} = -\rho_s\alpha_{ij}^{\text{VDW}} g_0^{\text{HS}}[\sigma_x;\zeta_x^{\text{eff}}(\lambda_{ij})] \quad \text{(A-8)}$$

where $g_{ij}^{\text{HS}}(\sigma_{ij};\zeta_3^{\text{eff}})$ is obtained from the Carnahan and Starling equation of state,[69]

$$g_0^{\text{HS}}[\sigma_x;\zeta_x^{\text{eff}}(\lambda_{ij})] = \frac{1 - \zeta_x^{\text{eff}}/2}{(1-\zeta_x^{\text{eff}})^3} \quad \text{(A-9)}$$

The effective packing fraction $\zeta_x^{\text{eff}}(\lambda_{ij})$ is obtained within the van der Waals one-fluid theory from the corresponding packing fraction of the mixture ζ_x given by,

$$\zeta_x^{\text{eff}}(\zeta_x,\lambda_{ij}) = c_1(\lambda_{ij})\zeta_x + c_2(\lambda_{ij})\zeta_x^2 + c_3(\lambda_{ij})\zeta_x^3 \quad \text{(A-10)}$$

where

$$\begin{pmatrix} c_1 \\ c_2 \\ c_3 \end{pmatrix} = \begin{pmatrix} 2.25855 & -1.50349 & 0.249434 \\ -0.669270 & 1.40049 & -0.827739 \\ 10.1576 & -15.0427 & 5.30827 \end{pmatrix}\begin{pmatrix} 1 \\ \lambda_{ij} \\ \lambda_{ij}^2 \end{pmatrix} \quad \text{(A-11)}$$

and

$$\zeta_x = \frac{\pi}{6}\rho_s\sigma_x^3 \quad \text{(A-12)}$$

with

$$\sigma_x^3 = \sum_{i=1}^{n}\sum_{j=1}^{n} x_{s,i}x_{s,i}\sigma_{ij}^3 = x_{s,1}^2\sigma_{11}^3 + 2x_{s,1}x_{s,2}\sigma_{12}^3 + x_{s,2}^2\sigma_{22}^3 \quad \text{(A-13)}$$

This corresponds to mixing rule MX1b in the original SAFT-VR approach for mixtures.[2]

The second-order perturbation term for the monomer excess free energy a_2 is expressed as:

$$a_2 = \sum_{i=1}^{n}\sum_{j=1}^{n} x_{s,i}x_{s,j}(a_2)_{ij} = x_{s,1}^2(a_2)_{11} + 2x_{s,1}x_{s,2}(a_2)_{12} + x_{s,2}^2(a_2)_{22} \quad \text{(A-14)}$$

where $(a_2)_{ij}$ is obtained through the local compressibility approximation:

$$(a_2)_{ij} = \frac{1}{2}K^{\text{HS}}\epsilon_{ij}\rho_s\frac{\partial(a_1)_{ij}}{\partial\rho_s} \quad \text{(A-15)}$$

and K^{HS} is the Percus−Yevick expression for the hard sphere isothermal compressibility,

$$K^{\text{HS}} = \frac{\zeta_0(1-\zeta_3)^4}{\zeta_0(1-\zeta_3)^2 + 6\zeta_1\zeta_2(1-\zeta_3) + 9\zeta_2^3} \quad \text{(A-16)}$$

Chain Contribution. The contact value of the radial distribution function $g_{ij}^{\text{HS}}(\sigma_{ij};\zeta_3)$ at the actual packing fraction ζ_3 is obtained from the expression of Boublik,[64]

$$g_{ij}^{\text{HS}}(\sigma_{ij};\zeta_3) = \frac{1}{1-\zeta_3} + 3\frac{D_{ij}\zeta_3}{(1-\zeta_3)^2} + 2\frac{(D_{ij}\zeta_3)^2}{(1-\zeta_3)^3} \quad \text{(A-17)}$$

where

$$D_{ij} = \frac{\sigma_{ii}\sigma_{jj}\sum_{i=1}^{n} x_{s,i}\sigma_{ii}^2}{(\sigma_{ii}+\sigma_{jj})\sum_{i=1}^{n} x_{s,i}\sigma_{ii}^3} = \frac{\sigma_{ii}\sigma_{jj}(x_{s,1}\sigma_{11}^2 + x_{s,2}\sigma_{22}^2)}{(\sigma_{ii}+\sigma_{jj})(x_{s,1}\sigma_{11}^3 + x_{s,2}\sigma_{22}^3)} \quad \text{(A-18)}$$

References and Notes

(1) Gil Villegas, A.; Galindo, A.; Whitehead, P. J.; Mills, S. J.; Jackson, G.; Burgess, A. N. *J. Chem. Phys*. **1997**, *106*, 4168.
(2) Galindo, A.; Davies, L. A.; Gil-Villegas, A.; Jackson, G. *Mol. Phys.* **1998**, *93*, 241.
(3) van Konynenburg, P. H.; Scott, R. L. *Philos. Trans. R. Soc. A* **1980**, *298*, 495.
(4) Scott, R. L.; van Konynenburg, P. H. *Discuss. Faraday Soc.* **1970**, *49*, 87.
(5) Graboski, M. S.; Daubert, T. E. *Ind. Eng. Chem. Process Des. Dev.* **1978**, *17*, 443.
(6) Graboski, M. S.; Daubert, T. E. *Ind. Eng. Chem. Process Des. Dev.* **1978**, *17*, 448.
(7) Nishiumi, H.; Arai, T.; Takeuchi, K. *Fluid Phase Equilib.* **1988**, *42*, 43.
(8) Moysan, J. M.; Paradowski, H.; Vidal, J. *Chem. Eng. Sci*. **1986**, *41*, 2069.
(9) Chapman, W. G.; Gubbins, K. E.; Jackson, G.; Radosz, M. *Fluid Phase Equilib.* **1989**, *52*, 31.
(10) Chapman, W. G.; Gubbins, K. E.; Jackson, G.; Radosz, M. *Ind. Eng. Chem. Res.* **1990**, *29*, 1709.
(11) Chapman, W. G.; Jackson, G.; Gubbins, K. E. *Mol. Phys*. **1988**, *65*, 1057.
(12) Wertheim, M. S. *J. Stat. Phys*. **1984**, *35*, 19.
(13) Wertheim, M. S. *J. Stat. Phys*. **1984**, *35*, 35.
(14) Wertheim, M. S. *J. Stat. Phys*. **1986**, *42*, 459.
(15) Wertheim, M. S. *J. Stat. Phys*. **1986**, *42*, 477.
(16) Muller, E. A.; Gubbins, K. E. *Ind. Eng. Chem. Res.* **2001**, *40*, 2193.
(17) Economou, I. G. *Ind. Eng. Chem. Res*. **2002**, *41*, 953.
(18) Gross, J.; Sadowski, G. *Fluid Phase Equilib.* **2000**, *168*, 183.
(19) Chen, S. S.; Kreglewski, A. *Ber. Bunsen-Ges.* **1977**, *81*, 1048.
(20) Garcia-Sanchez, F.; Eliosa-Jimenez, G.; Silva-Oliver, G.; Vazquez-Roman, R. *Fluid Phase Equilib.* **2004**, *217*, 241.
(21) McCabe, C.; Galindo, A.; Gil-Villegas, A.; Jackson, G. *Int. J. Thermophys.* **1998**, *19*, 1511.
(22) McCabe, C.; Gil-Villegas, A.; Jackson, G. *J. Phys. Chem. B* **1998**, *102*, 4183.
(23) McCabe, C.; Jackson, G. *Phys. Chem. Chem. Phys*. **1999**, *1*, 2057.
(24) McCabe, C.; Galindo, A.; Garcia-Lisbona, M. N.; Jackson, G. *Ind. Eng. Chem. Res.* **2001**, *40*, 3835.
(25) McCabe, C.; Kiselev, S. B. *Ind. Eng. Chem. Res*. **2004**, *43*, 2839.
(26) McCabe, C.; Kiselev, S. B. *Fluid Phase Equilib*. **2004**, *219*, 3.
(27) Galindo, A.; Florusse, L. J.; Peters, C. J. *Fluid Phase Equilib*. **1999**, *160*, 123.
(28) Filipe, E. J. M.; de Azevedo, E.; Martins, L. F. G.; Soares, V. A. M.; Calado, J. C. G.; McCabe, C.; Jackson, G. *J. Phys. Chem. B* **2000**, *104*, 1315.
(29) Filipe, E. J. M.; Martins, L. F. G.; Calado, J. C. G.; McCabe, C.; Jackson, G. *J. Phys. Chem. B* **2000**, *104*, 1322.
(30) McCabe, C.; Galindo, A.; Garcia-Lisbona, M. N.; Jackson, G. *Ind. Eng. Chem. Res*. **2001**, *40*, 3835.
(31) Sun, L. X.; Zhao, H. G.; Kiselev, S. B.; McCabe, C. *Fluid Phase Equilib.* **2005**, *228*, 275.
(32) Sun, L. X.; Zhao, H. G.; Kiselev, S. B.; McCabe, C. *J. Phys. Chem. B* **2005**, *109*, 9047.
(33) McCabe, C.; Galindo, A.; Gil-Villegas, A.; Jackson, G. *J. Phys. Chem. B* **1998**, *102*, 8060.
(34) Bonifacio, R. P.; Filipe, E. J. M.; McCabe, C.; Gomes, M. F. C.; Padua, A. A. H. *Mol. Phys*. **2002**, *100*, 2547.
(35) Galindo, A.; Burton, S. J.; Jackson, G.; Visco, D. P.; Kofke, D. A. *Mol. Phys.* **2002**, *100*, 2241.
(36) McCabe, C.; Galindo, A.; Cummings, P. T. *J. Phys. Chem. B* **2003**, *107*, 12307.
(37) Galindo, A.; Gil-Villegas, A.; Whitehead, P. J.; Jackson, G.; Burgess, A. N. *J. Phys. Chem. B* **1998**, *102*, 7632.
(38) Blas, F. J.; Galindo, A. *Fluid Phase Equilib.* **2002**, *194*−*197*, 501.
(39) Galindo, A.; Blas, F. J. *J. Phys. Chem. B* **2002**, *106*, 4503.
(40) Colina, C. M.; Galindo, A.; Blas, F. J.; Gubbins, K. E. *Fluid Phase Equilib*. **2004**, *222*, 77.
(41) Colina, C. M.; Gubbins, K. E. *J. Phys. Chem. B* **2005**, *109*, 2899.
(42) Galindo, A.; Gil-Villegas, A.; Jackson, G.; Burgess, A. N. *J. Phys. Chem. B* **1999**, *103*, 10272.
(43) Gil-Villegas, A.; Galindo, A.; Jackson, G. *Mol. Phys.* **2001**, *99*, 531.
(44) Patel, B. H.; Paricaud, P.; Galindo, A.; Maitland, G. C. *Ind. Eng. Chem. Res.* **2003**, *42*, 3809.
(45) Buenrostro-Gonzalez, E.; Lira-Galeana, C.; Gil-Villegas, A.; Wu, J. *AIChE J*. **2004**, *50*, 2552.
(46) Stell, G.; Rasaiah, J. C.; Narang, H. *Mol. Phys.* **1972**, *23*, 393.
(47) Deutch, J. M. *Annu. Rev. Phys. Chem*. **1973**, *24*, 301.
(48) Stell, G.; Rasaiah, J. C.; Narang, H. *Mol. Phys*. **1974**, *27*, 1393.
(49) Gubbins, K. E.; Twu, C. H. *Chem. Eng. Sci.* **1978**, *33*, 863.
(50) Verlet, L.; Weis, J. J. *Mol. Phys*. **1974**, *28*, 665.
(51) Vimalchand, P.; Donohue, M. D. *Ind. Eng. Chem. Fundam.* **1985**, *24*, 246.
(52) Donohue, M. D.; Prausnitz, J. M. *AIChE J*. **1978**, *24*, 849.
(53) Saager, B.; Fischer, J. *Fluid Phase Equilib*. **1992**, *72*, 67.
(54) Gross, J. *AIChE J*. **2005**, *51*, 2556.
(55) Benavides, A. L.; Guevara, Y.; del Río, F. *Physica A* **1994**, *202*, 420.
(56) del Río, F.; Benavides, A. L.; Guevara, Y. *Physica A* **1995**, *215*, 10.
(57) Guevara, Y.; Benavides, A. L.; del Río, F. *Mol. Phys.* **1996**, *89*, 1277.
(58) Gil-Villegas, A.; del Rìo, F.; Benavides, A. L. *Fluid Phase Equilib*. **1996**, *119*, 97.
(59) Benavides, A. L.; Guevara, Y.; Estrada-Alexanders, A. F. *J. Chem. Thermodyn.* **2000**, *32*, 945.
(60) Guevara, Y.; Benavides, A. L.; Estrada-Alexanders, A. F.; Romero, M. *J. Phys. Chem. B* **2000**, *104*, 7490.
(61) Benavides, A. L.; Guevara, Y. *J. Phys. Chem. B* **2003**, *107*, 9477.
(62) Gray, C. G.; Gubbins, K. E. *Theory of Molecular Fluids: Fundamentals*; Clarendon Press: Oxford, 1984; Vol. 1.
(63) Leonard, P. J.; Henderson, D.; Barker, J. A. *Trans. Faraday Soc.* **1970**, *66*, 2439.
(64) Boublik, T. *J. Chem. Phys*. **1970**, *53*, 471.
(65) Mansoori, G. A.; Carnahan, N. F.; Starling, K. E.; Leland, T. W. *J. Chem. Phys*. **1971**, *54*, 1523.
(66) Larsen, B.; Rasaiah, J. C.; Stell, G. *Mol. Phys.* **1977**, *33*, 987.
(67) Hansen, J. P.; McDonald, I. R. *Theory of Simple Liquids*, 2nd ed.; Academic Press: London, 1986.
(68) Hoye, J. S.; Lebowitz, J. L.; Stell, G. *J. Chem. Phys*. **1974**, *61*, 3253.
(69) Carnahan, N. F.; Starling, K. E. *J. Chem. Phys.* **1969**, *51*, 635.
(70) Nowak, P.; Kleinrahm, R.; Wagner, W. *J. Chem. Thermodyn*. **1997**, *29*, 1137.
(71) Kidnay, A. J.; Miller, R. C.; Parrish, W. R.; Hiza, M. *J. Cryog.* **1975**, *15*, 531.
(72) Stryjek, R.; Chappele, P. S.; Kobayash, R. *J. Chem. Eng. Data* **1974**, *19*, 334.
(73) Brown, T. S.; Niesen, V. G.; Sloan, E. D.; Kidnay, A. J. *Fluid Phase Equilib*. **1989**, *53*, 7.
(74) Kalra, H.; Robinson, D. B.; Besserer, G. J. *J. Chem. Eng. Data* **1977**, *22*, 215.
(75) Llave, F. M.; Chung, T. H. *J. Chem. Eng. Data* **1988**, *33*, 123.
(76) Llave, F. M.; Luks, K. D.; Kohn, J. P. *J. Chem. Eng. Data* **1985**, *30*, 435.
(77) Wisotzki, K. D.; Schneider, G. M. *Ber. Bunsen-Ges.* **1985**, *89*, 21.
(78) Hicks, C. P.; Young, C. L. *Chem. Rev.* **1975**, *75*, 119.
(79) Stryjek, R.; Chappele, P. S.; Kobayash, R. *J. Chem. Eng. Data* **1974**, *19*, 340.
(80) Yu, P.; Elshayal, I. M.; Lu, B. C. Y. *Can. J. Chem. Eng.* **1969**, *47*, 495.
(81) Grauso, L.; Fredenslund, A.; Mollerup, J. *Fluid Phase Equilib*. **1977**, *1*, 13.
(82) Gupta, M. K.; Gardner, G. C.; Hegarty, M. J.; Kidnay, A. J. *J. Chem. Eng. Data* **1980**, *25*, 313.
(83) Zeck, S.; Knapp, H. *Fluid Phase Equilib*. **1986**, *25*, 303.
(84) Wirths, M.; Wisotzki, K. D. *Ber. Bunsen-Ges*. **1984**, *88*, 921.
(85) Zhao, H.; McCabe, C. *J. Chem. Phys.* **2006**, *125* (10), 4504.